JACOBS PUBLISHERS

OPEN ACCESS

Jacobs Journal of Ophthalmology

Research Article

Retinal Ganglion Cell Death is correlated with Eyeball Expansion in Mammals

Ji-Jie Pang[1*], Samuel M. Wu[1]

[1]*Department of Ophthalmology, Baylor College of Medicine, One Baylor Plaza, NC 205, Houston, Texas 77030, USA*

**Corresponding author: Dr. Ji-Jie Pang, M.D., Ph.D. Department of Ophthalmology, Baylor College of Medicine, One Baylor Plaza, NC 205, Houston, Texas 77030, USA; Tel: (713) 798 4349; Fax: (713) 798 6457; Email: jpang@bcm.edu*

Received: 10-09-2014

Accepted: 11-24-2014

Published: 02-06-2015

Abstract

Retinal ganglion cells (GCs) are gradually damaged in glaucoma patients and old subjects. It is unclear how mechanical stress (IOP) and strain (global expansion) differentially contribute to the progressive GC death. To further understand such retinal GC damage, neuronal populations in the GC layer (GCL) were studied in DBA/2J (D2) and wild type mice (1.5 to 19 months), in conjunction with observation of eyeball volume, IOP and the effect of anesthesia on IOP. The entire retinal GC population was retrograde-labeled and observed with a confocal microscope. The results showed that GCs and TO-PRO-3-identified total neurons in the GCL were dramatically decreased with age in D2 mice, and displaced amacrine cells (ACs) were reduced moderately. D2 mice possessed significantly fewer GCs, displaced ACs and total neurons in the GCL compared to wild type mice. Eyeball volume was significantly enlarged with age. The eyeball expansion was asymmetric and severe in D2 mice compared to that in wild type mice. After intraperitoneal anesthesia injection IOP was decreased in some D2 mice and increased in some wild type mice, which was, however, not statistically significant. GC populations were significantly negatively correlated with eyeball volume in D2 mice but not in wild type mice. It is concluded that eyeball expansion is pathologic in D2 mice, which cannot be ruled out for mediating GC death in glaucoma and old subjects.

Keywords: Retina; Neuronal degeneration; Glaucoma; Mouse; Displaced Amacrine Cells

Abbreviations

GC: Ganglion Cell;
GCL: GC Layer;
AC: Amacrine Cell;
NB: Neurobiotin;
D2: DBA/2J;
B6: C57BL/6J;
EV: Eyeball Volume;
IOP: Intraocular Pressure

Introduction

Glaucoma is a family of multifactorial neuropathies characterized by loss of retinal ganglion cells (GCs). It is a leading cause of blindness worldwide [1,2] but its exact pathological mechanism is unclear. Glaucomatous GC damage may present with eyeball expansion (e.g. congenital glaucoma) [3,4] and high or normal intraocular pressure (IOP) (high- or normal-tension glaucoma) [5-9] . It is unclear how mechanical stress (IOP) and strain (global expansion) contribute to the

progression of GC death [1,10-12]. Improving outflow of aqueous humor has been the only proven way of preventing the onset and progression of glaucoma [13-15]. Such treatment apparently modifies IOP and it seems less likely not to influence eyeball volume (EV). However, data on EV alterations in glaucoma is still missing.

IOP is the major risk factor for high-tension glaucoma [13,14]. But it is not accountable for all glaucoma cases. A significant number of patients with normal IOP develop glaucoma [11-15], while other individuals with elevated IOP show no signs of the disease (ocular hypertension). Optic disk cupping is a common clinical symptom of glaucoma. Normal- and high-tension glaucoma patients [5-9] often share similar optic disc and visual field appearances. Normal-tension glaucoma was first described in 1857 by Von Graefe. Its pathological mechanism is not clear. It consists of typical glaucomatous disc and field changes, an open angle and pressures within the statistically normal range [16-20]. IOP asymmetry in these patients is not related to visual field asymmetry [21]. Systematic blood pressure and intracranial pressure [22,23] appear to be related to normal tension glaucoma, yet the data are still highly conflicting [17,20,22,23]. Ischemia was also reported to be responsible for the optic nerve damage in normal-tension glaucoma patients who suffered migraine [24], shock, blood loss, low blood pressure and optic disc hemorrhages [17,18]. Congenital glaucoma is a subtype of glaucoma in children, which is characterized by early GC death, elevation of IOP and dramatically enlarged eyeball and cornea [3,4].

We have previously established a method for retrograde-labeling of all GCs in the mouse retina. Its specificity and efficiency for labeling the entire GC population has been examined and confirmed [25,26]. Using this technique, in conjunction with confocal microscopy and immunofluorescence, we compared GC death and some related factors in wild type mice and glaucoma-prone DBA/2J mice. The study was focused on: 1) GC populations, amacrine cell (AC) populations and total neurons in the retinal GC layer (GCL) in the two strains of mice; 2) EV and its relation to neuron counts in the GCL; and 3) the effect of anesthesia on IOP and the relation of IOP to neuron populations in the GCL.

Materials and Methods

Animals

All procedures in this study followed the NIH animal care guidelines and were approved by the Baylor College of Medicine Animal Care and Use Committee. The animals used in this study were DBA/2J (D2) and C57BL/6J (B6) mice purchased from Jackson Laboratory (Bar Harbor, ME, USA). D2 mice develop glaucoma associated with iris stromal atrophy and iris pigment dispersion phenotypes. Genetic studies documented by the vendor defined two separate loci that contribute to the overall phenotype in the D2 mouse, ipd (iris pigment dispersion) and isa (iris stromal atrophy), and either mutation in a homozygous state contributes to glaucoma. Glaucoma is a chronic disease. It is more prevalent in aging populations, but it also occurs in children. Whether the pathological mechanism is the same in these two age spans is not clear. To investigate basically how eyeball dimension changes with age and how the change is related to GC loss or glaucoma, we, thus, monitored the eyeball size in a wide life span. 1.5- to 19- month-old mice, males and females were included. We randomly selected healthy mice at desired ages for the experiment without IOP restriction. All mice were dark-adapted for 1 to 2 hours prior to the experiment. Animals were anesthetized with an intra-peritoneal injection of ketamine (200 mg/kg) and xylazine (10 mg/kg). IOP was measured with a TonoLab rebound tonometer [27] (Colonial Medical Supply, Franconia, NH) 10 minutes after the anesthesia injection. Each IOP value was based on three measurements and each measurement was averaged from 5 trials. The eyes were enucleated after the animals were deeply anesthetized. Animals were euthanatized by over-dose of the anesthesia.

Retrograde labeling of GCs

Previously established techniques [26] were precisely followed. Animals were dark-adapted and eyeballs were enucleated under the illumination of dim red light. A mixture of neurobiotin, a gap-junction-permeable dye (NB, MW 322.85, Vector Laboratories, Burlingame, CA), and Lucifer yellow, a less permeable dye (LY, MW 457.24; Sigma-Aldrich, St. Louis, MO) [28-30], was used for the labeling. The fixed retinas were blocked with 10% donkey serum (Jackson ImmunoResearch, West Grove, PA) in TBS (D-PBS with 0.5% Triton X-100 (Sigma-Aldrich) and 0.1% NaN3 (Sigma-Aldrich)) for 1 hour at room temperature or at 4°C overnight to reduce nonspecific labeling.

Retinas and free-floating sections were incubated in primary antibodies in the presence of 3% donkey serum-TBS for 3 to 5 days at 4°C. Controls were also processed without primary antibodies. Following several rinses, the slices and whole retinas were then transferred into Cy3-, Cy5-, or Alexa Fluor 488-conjugated streptavidin (1:200, Jackson ImmunoResearch), with Cy3- and/or Cy5-conjugated secondary antibodies (1:200, Jackson ImmunoResearch) and/or Alexa Fluor 488-conjugated secondary antibodies (1:200; Molecular Probes, Eugene, OR), in 3% normal donkey serum-TBS solution at 4°C overnight. A nuclear dye, TO-PRO-3 (0.5 μL/mL, Molecular Probes) was used with the secondary antibody to visualize nuclei in retinas [26]. After extensive rinsing, the retinal preparations were cover-slipped. Two small pieces of filter paper (180-μm thick, MF-membrane filters; Millipore, Billerica, MA) were mounted beside whole retinas to prevent them from being

over-flattened. Consistent labeling was obtained from both slice preparations and whole retinas, in line with previous reports [26, 31].

Eyeball measurement

Eyeballs were measured for EV immediately after dissection. Soft tissues and blood on the eyeballs were carefully and completely removed. The eyeball exterior dimensions were measured with 40X amplification with a Zeiss microscope and a graduated lens. The globe diameter in x-y dimension (coronal plane) and that in y-z dimension (sagittal plane) were measured for calculation of the average radius and eyeball volume (EV).

Identification and counting of GCs, displaced ACs and total neurons in the GCL

We have previously shown that the double retrograde labeling technique was reliable and specific for visualization of the entire retinal GC population [25,26]. The somas in the GCL, IPL and INL that contained LY were identified as GCs. All GC somas, thereby identified, contained NB and thus all GC somas were positive for both LY and NB. But NB labeled more somas than LY did. These NB-labeled LY- negative somas, often weakly NB positive, were identified as GC-coupled neurons. They comprised nearly 11% of the displaced ACs [26]. A confocal microscope and retrograde- identified axonal bundles were critical for us to accurately locate the GCL (see results), especially for retinas with few GC somas survived.

TO-PRO-3 labeled all nuclei in the retina. The total TO-PRO-3 labeled nuclei in the GCL, excluding those from non-neurons [26], were counted as total neurons there. Total displaced ACs was calculated by deducting the total GC number from the total neuron number in the GCL. Total displaced ACs in wild-type mice revealed previously in the same experimental condition comprise 56% of the total neurons in the GCL [26].

Retinal preparations were observed with a laser scanning confocal microscope (LSM 510, Carl Zeiss, Germany), and LSM software was used to take images. Images were further processed in Adobe Photoshop v9.0.2 for presentation purposes. For better visibility, some images (or panels) were inverted or presented in black and white.

Previously published methods [25,26] were closely followed for counting neurons. Neurons in the GCL were usually arranged in a single layer in the mouse retina. They were counted in flat-mounted whole retinas. The total number (N) of GCs was obtained either by counting all GCs in the GCL or calculated by N= S * D, where D is the planar density of the somas, sampled evenly in around 10% surface area of a whole-mount retina including the peripheral and central retina [26], and S is the total surface area of a whole-mount retina measured with a Zeiss microscope in vitro with 40X amplification and a graduated lens. The total neurons and displaced ACs in the GCL were counted similarly.

Data Analysis

Data are presented as mean ± standard error (s.e.) of the mean. The difference between data groups was analyzed by two-tail student *t*-test. Correlations among data groups were analyzed with Microsoft Excel 2007 and Sigma Plot 11.2. The α level for accepting statistical significance was 0.05.

Results

Age-related change in neuronal populations in the mouse retina

Figure 1 shows a dramatic reduction of GC counts in a whole-mount adult D2 retina. Displaced AC counts, calculated by total neurons minus GC counts, are also reduced. The statistic data on changes in GC and AC populations with age are reported in Figure 2. The data are plotted as neuronal populations against the age in figure 2A for wild type mice and figure 2B for D2 mice. Average neuronal populations in the two strains of mice are presented with a bar chart in figure 2C.

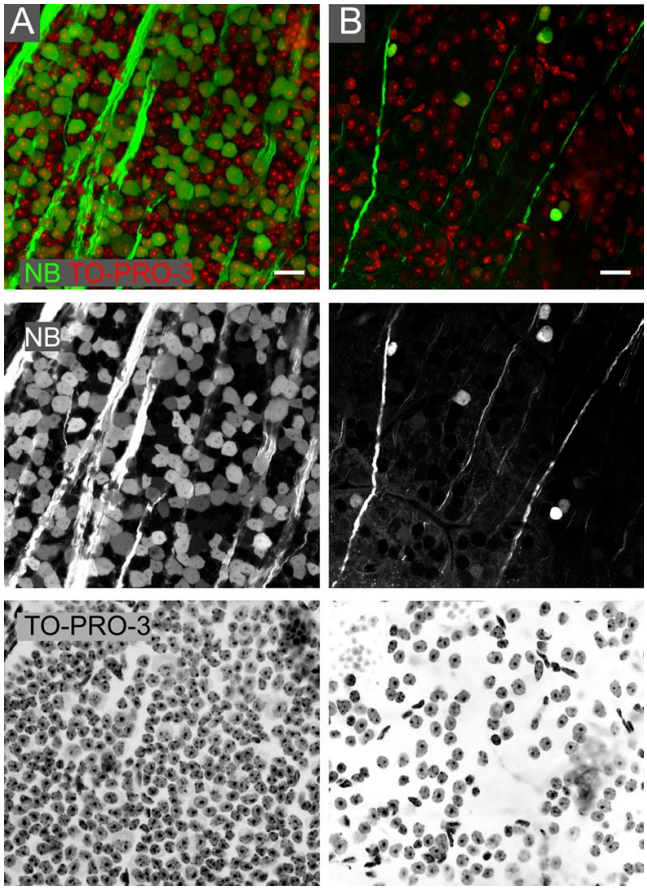

Figure 1. Selective GC soma death in the D2 mouse. Confocal micrographs are taken from the GCL in flat-mounted retinas retrogradely labeled by NB and stained by a nuclear dye TO-PRO-3. The red and green channels of the top panel images are separately depicted in the middle and bottom panels. Retrograde-labeled GCs (green in upper panels and white in middle panels) in the peripheral retina is largely reduced in an adult D2 mouse (B, 10-month-old), compared to a healthy young D2 mouse (A, 4-month-old). TO-PRO-3-revealed neurons (red in upper panels and black in bottom panels) in the GCL in B are largely reduced, compared to those in A. It indicates selective GC death and moderate loss of displaced ACs in the adult D2 mouse. NB, neurobiotin; GC, ganglion cell; GCL, GC layer; ACs, amacrine cells; D2, DBA/2J; scale bar, 20μm

In wild type mice (22 retinas), GCs, ACs and total neurons in the GCL were not clearly changed with the age (all p>0.5). In D2 mice (51 retinas), GCs (p<0.0001), ACs (p=0.010) and total neurons (p=0.0007) in the GCL were significantly negatively correlated with the age (Figure 1 and 2), and their populations were all significantly smaller compared to those in wild type mice (all p<0.0001).

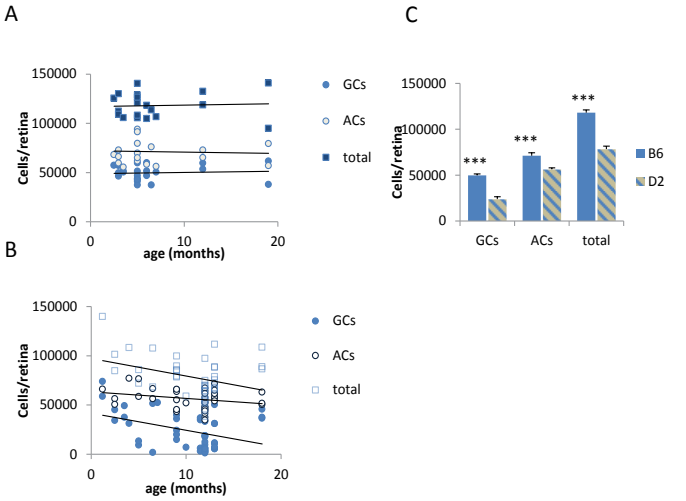

Figure 2. Age-related changes in GC populations in the mouse retina. In wild type mice (A) neuron counts in the GCL are not correlated with the age. In D2 mice (B) GCs (p<0.0001) and total neuron populations (p=0.0007) in the GCL are negatively correlated with the age, and AC counts in the GCL are moderately reduced with the age (p=0.010). GCs, ACs and total neurons in the GCL are fewer in D2 mice compared to B6 mice (C). ***: p≤0.0001 (between two stains); D2, DBA/2J; B6, C57BL/6J; GCs, ganglion cells; GCL, GC layer; ACs, amacrine cells.

Age-related change in eyeball volume

The data on EV is reported in figure 3 and 4. Individual EV is firstly plotted against the age in figure 3A, in order to reveal age-related change. Furthermore, averaged EV is plotted with a bar chart in figure 3B for easier comparison between the two strains of mice. Eyeball expansion in adult mice was not only statistically significant, but also detectable by naked eyes, especially in the animals with asymmetric eyeball expansion. (Figure. 4).

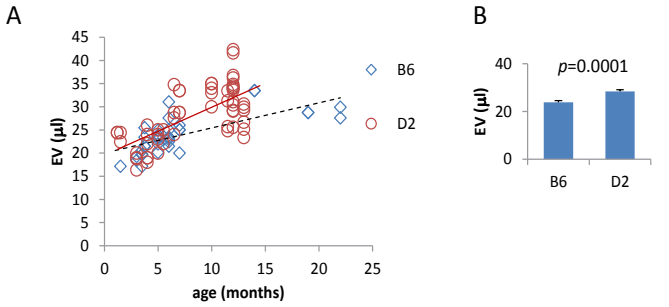

Figure 3. Age-related eyeball expansion. EV is plotted against age in A. And the average EV is depicted by a bar chart in B. In both wild type and D2mice, EV was positively correlated with age (A). Age-related increase of EV is more severe in D2 mice (solid line) than in wild type mice (dash line) (A). Average EV in D2 mice is significantly larger than that in wild type mice (B). EV, eyeball volume; D2, DBA/2J; B6, C57BL/6J.

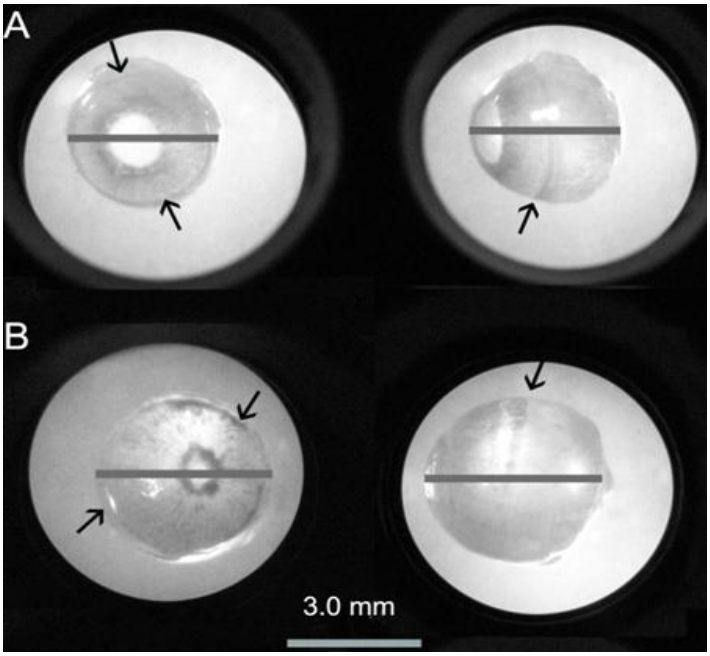

Figure 4. Eyeball expansion in the adult D2 mouse. Front-view (left panels) and side-view (right panels) images of eyeballs from D2 mice (A, 4-month-old; B, 10-month-old) were taken from an infrared-illuminated dissecting microscope. Eyeballs are encircled by the bright background illumination. Bars superimposed on the eyeballs denote diameters. The eyeballs show nearly spherical shape. The eyeball in B has a large volume, large cornea but smaller pupil. Arrows indicate the edge of the cornea, where a shallow indention is visible in the young D2 mouse but nearly absent in the adult D2 mouse. EV, eyeball volume; D2, DBA/2J.

For wild type (37 eyeballs) and D2 mice (61 eyeballs), EV was positively correlated with age (both p<0.0001). But the age-related increase in EV was more severe in D2 mice than in wild type mice (Figure. 3 and 4). EV in fellow eyeballs was asymmetric in many adult D2 mice. The enlarged D2 eyeballs usu-

ally showed a smaller pupil, large cornea and a shallower or diminished indentation at corneoscleral junction.

Relationship between GC populations and eyeball volume

We studied EV and GC populations in the same eyeballs. In Figure 5, the entire GC population for each retina is presented in a scatter plot as a function of EV. GC populations in D2 mice display a large variation, in consistent to the known variation of glaucoma vulnerability among mice in this strain [32], while GC populations in wild type mice display a much smaller variation. GC populations in wild type mice do not alter with EV ($p>0.5$). But in D2 mice GC populations are negatively correlated with EV ($p<0.0001$) (Figure 5).

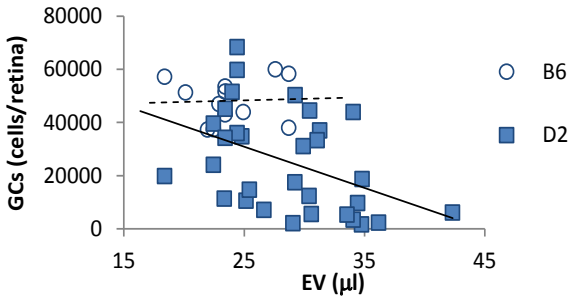

Figure 5. Relation between GC population and EV. GC counts are plotted in a scatter plot against EV. GC populations in wild type mice are not altered with EV (dash line), while GCs were negatively correlated with EV in D2 mice (solid line). EV, eyeball volume; D2, DBA/2J; B6, C57BL/6J.

Intraocular pressure and the effect of anesthesia

We monitored IOP on age-matched D2 and wild type mice at successive time points after injection of anesthesia, in order to clarify the influence of anesthesia on the results. The observation began immediately after the injection and terminated at 25 minutes after the injection. The data are firstly presented as scatter plots in figure 6B for wild type mice and 6A for D2 mice. To show the distribution or variation of the anesthesia induced IOP fluctuation among the animals, maximum IOP changes (ΔIOP_{max}) was calculated by the highest IOP value minus the lowest value for each mouse and the data was presented in a histogram (Fig. 6C). The average IOP levels in D2 and wild type mice were further compared before and after 450 seconds of anesthesia injection (Figure. 6D).

The data showed that IOP was slightly enhanced by the anesthesia in some wild type mice (Figure. 6B) but moderately reduced in some D2 mice (Figure. 6A) (3.5 to 6.5-month-old for both strains). Yet, the general effect was lack of statistical significance ($p>0.05$) (Figure. 6D). The maximum anesthesia-induced IOP fluctuation was distributed around a mean of ~10 mmHg (Figure. 6C).

Based on above observation, IOP measurement that was associated with the study of GC populations was performed around 10 minutes after intraperitoneal injection of anesthesia. Thus, the experimental results were not to be significantly altered by anesthesia. IOP is plotted in a scatter plot (Figure. 6E) against age. Wild type and D2 mice both show large IOP variation (ranged 10-35 mmHg) (Figure. 6E), while IOP is more dispersed for adult D2 mice than adult wild type mice.

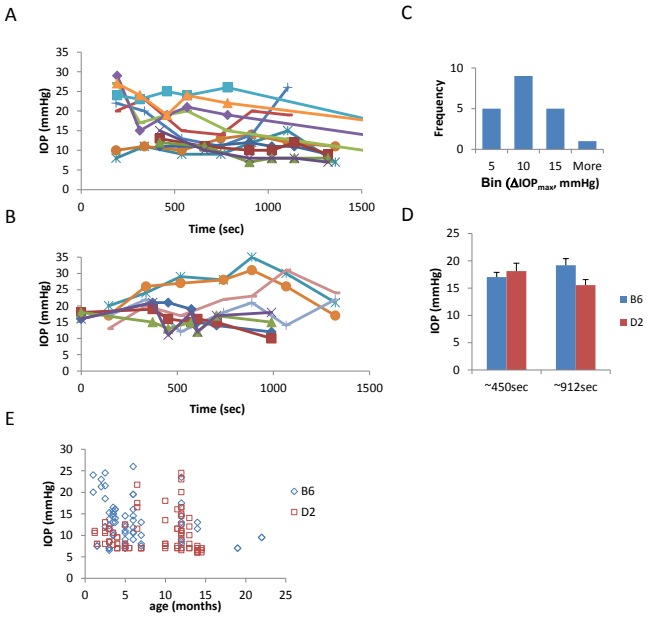

Figure 6. IOP measurement in D2 and B6 mice and the effect of anesthesia on IOP. IOP is monitored. IOP values are plotted against time in scatter plots (A, B). Each color line in A and B connects data points from an individual eyeball. The maximum IOP fluctuation from each eyeball is further presented within a histogram (C) to show its distribution. Anesthesia-induced IOP changes are further analyzed within two temporal windows (D). IOP data obtained from all mice associated with study of GCs are reported in E. The influence of anesthesia on IOP varies among eyeballs and mouse strains. IOP is moderately reduced in some D2 mice (A) but slightly enhanced by the anesthesia in some wild type mice (B). Yet, IOP after 450 seconds of anesthesia injection was not significantly different from that before 450 seconds (D) in both stains of mice. The maximum IOP fluctuations induced by the anesthesia are distributed around a mean of ~10 mmHg (C). IOP in wild type and D2 mice measured 10 minutes after anesthesia injection shows similarly large variation (E). D2, DBA/2J; B6, C57BL/6J.

Relationship between GC populations and IOP

In Figure 7, GC populations are plotted against IOP. Each data point represents one retina. GC populations in wild type mice are not related to IOP levels in the age span observed, while that in D2 mice shows a large variation, consistent to the diversity of glaucoma vulnerability among mice in this strain. In wild type mice, GC populations were positively correlated with IOP ($p<0.0001$). In D2 mice GC populations tended to reduce

with IOP elevation (but p=0.426).

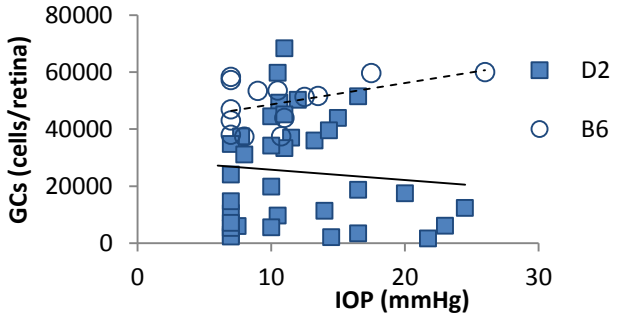

Figure 7. IOP and its relation to GC populations. GC counts are plotted against IOP. The scatter plots show that GC populations are positively correlated with IOP in wild type mice (dash line) but tend to reduce with IOP elevation in D2 mice (solid line). D2, DBA/2J; B6, C57BL/6J.

Discussions

D2 mice, in contrast to wild type mice, suffer unique ocular pathology and progressive retinal GC death

Ocular environment is subject to pressure and volume changes due to fluctuation of aqueous humor and other physiological and pathological factors [33,34]. Yet, eyeball volume has not been documented in the mice. And its role in glaucoma is unknown. Our data showed that eyeball volume increased with age in the mouse, which was moderated in wild type mice but severe and asymmetric in D2 mice. It suggests that eyeball expansion in D2 mice is pathologic instead of normal growth. This idea is in line with significant GC loss in D2 retinas [35-39].

In D2 mice neurons in the GCL are reduced with age, which is well consistent in our results and previous findings [35-39]; but GC populations have not been studied simultaneously with displaced ACs and total neurons in D2 retinas. For the human glaucoma, it is still unclear how GC soma death and axonal damage differentially contribute to vision loss [12,18,40-43]. By simultaneous observation of all neuronal populations in the GCL, we found that total neurons decreased parallelly with GC counts, while displaced ACs were not increased with age. The results confirm that GC somas gradually die with age in glaucoma model mice. It further suggests that GC soma death may contribute to earlier vision loss in glaucoma model mice.

Eyeball expansion may be related to GC death in glaucoma mouse models

In line with buphthalmos found in congenital glaucoma patients [4], our data demonstrate for the first time that ocular expansion is present in glaucoma mouse models and old wild type mice. D2 mice showed more severe eyeball expansion than wild type mice, and fellow eyeballs suffer asymmetric enlargement. The indentation at corneoscleral junction in the enlarged eyeballs was diminished. Therefore, eyeball expansion in D2 mice is likely to be pathologic instead of normal growth. Although an initial harmful global expansion is presumably to be compensated by remodeling of the eyeball shell, but the remodeling, if any, is expected to occur slowly and behind the expansion. Thus, it cannot guaranty that no GC is damaged by the initial mechanical stretches. Therefore, global expansion is hardly ruled out for mediating GC death.

Accumulation of aqueous humor seems to be able to induce eyeball expansion, as water is nearly uncompressible under clinical IOP levels [44-46] . Yet it is unclear how accumulation of aqueous humor affects eyeball volume or how IOP and eyeball volume interacts with each other [33,34,47]. Our data and previous results [38] indicate accumulation of aqueous humor in D2 mice, which may well interpret eyeball expansion that we observed in this paper. Pathologic eyeball expansion appears to be a novel mechanism that may mediate retinal GC damage. Glaucoma with normal IOP has been known for more than a century [16-20]. It is worthy to note that in both human glaucoma patients and animals suffering glaucoma-like retinal degeneration, IOP elevation does not always accompany retinopathy. It is neither a definite indicator for retinal pathology [21] nor a sole mechanism for glaucoma [22,40,41,48]. D2 mice show high or normal IOP from 2-19 months of age [32, 38]. Our data, in line with previous reports [32,38,49] reveal GC loss and IOP elevation in some mice around 10 months of age. IOP often peaks around 10 months of ages in D2 mice and reduced afterwards [38,50], while GC populations, once lost, cannot be recovered. These non-parallel changes may partially explain the insignificant negative correlation between IOP and GC counts between 1.5-19 months of age in this study. The other possible reason is that IOP itself fluctuates extensively [33,51,52], even in the matter of seconds. The fluctuation tends to make IOP values measured discontinuously less consistent.

Nevertheless, current glaucoma study appears to face two major problems, one is to decode the IOP elevation-related glaucoma, and the other is to explain glaucoma pathology without IOP elevation. Data obtained from both directions are likely to give us a better overview of glaucoma.

Eyeball expansion can be a factor mediating a variety of glaucoma phenotypes

Glaucoma patients may have high or normal levels of IOP, while congenital glaucoma patients suffer both IOP elevation and eyeball expansion [3,4]. Similar to the human, D2 mice show enlarged eyeballs, as well as high or normal IOP from 2-19 months of age [32,38]. Selective GC damage is a common pathology in patients with high-tension glaucoma, normal-tension glaucoma and congenital glaucoma, but no known mechanism may universally explain the pathogenesis in these glaucoma phenotypes [11,17-20,53,54].

The pathological diversity in D2 mice resembles the variety of human glaucoma, implying that GC damage in these glaucoma conditions probably shares certain mechanisms. Eyeball expansion-related anatomical alterations have been reported previously in glaucoma, including large eyeballs and cornea in congenital glaucoma patients [3,4], optic disk cupping in high- and normal-tension glaucoma patients, retinal expansion [50] and inner retinal thinning [39] in D2 mice, enlarged laminar pores [55] and stretch-sensitive activation of astrocytes [56,57] in glaucoma patients. Our data, in conjunction with previous studies, suggests that retinal-expansion is possibly a retinal pathology shared by a variety of glaucoma phenotypes.

Conclusions

GCs progressively die with age in D2 mice. Eyeball volume is pathologically expanded with age in D2 mice, which is correlated to GC loss. Eyeball expansion, thus, cannot be ruled out for mediating GC death in glaucoma.

Acknowledgements

We thank Dr. Roy Jacoby for critical reading this manuscript. This work is supported by Grants from NIH (EY 04446), NIH (EY 019908), NIH Vision Core (02520), the Retina Research Foundation (Houston), and Research to Prevent Blindness, Inc.

References

1. Coleman AL, Brigatti L. The glaucomas. Minerva Med. 2001, 92(5): 365-379.

2. Quigley HA, Vitale S. Models of open-angle glaucoma prevalence and incidence in the United States. Invest Ophthalmol Vis Sci. 1997, 38(1): 83-91.

3. Ho CL, Walton DS. Primary megalocornea: clinical features for differentiation from infantile glaucoma. J Pediatr Ophthalmol Strabismus. 2004, 41(1): 11-17.

4. Papadopoulos M, Cable N, Rahi J, Khaw PT. The British Infantile and Childhood Glaucoma (BIG) Eye Study. Invest Ophthalmol Vis Sci. 2007, 48(9): 4100-4106.

5. Lewis RA, Hayreh SS, Phelps CD. Optic disk and visual field correlations in primary open-angle and low-tension glaucoma. Am J Ophthalmol. 1983, 96(2): 148-152.

6. Motolko M, Drance SM, Douglas GR. Visual field defects in low-tension glaucoma. Comparison of defects in low-tension glaucoma and chronic open angle glaucoma. Arch Ophthalmol. 1982, 100(7): 1074-1077.

7. King D, Drance SM, Douglas G, Schulzer M, Wijsman K. Comparison of visual field defects in normal-tension glaucoma and high-tension glaucoma. Am J Ophthalmol. 1986, 101(2): 204-207.

8. Miller KM, Quigley HA. Comparison of optic disc features in low-tension and typical open-angle glaucoma. Ophthalmic Surg. 1987, 18(12): 882-889.

9. Iester M, Mikelberg FS. Optic nerve head morphologic characteristics in high-tension and normal-tension glaucoma. Arch Ophthalmol. 1999, 117(8): 1010-1013.

10. Fechtner RD, Weinreb RN. Mechanisms of optic nerve damage in primary open angle glaucoma. Surv Ophthalmol. 1994, 39(1): 23-42.

11. Bouhenni RA, Dunmire J, Sewell A, Edward DP. Animal models of glaucoma. J Biomed Biotechnol. 2012, 2012: 692609.

12. Caprioli J, Coleman AL. Blood pressure, perfusion pressure, and glaucoma. Am J Ophthalmol. 2010, 149(5): 704-712.

13. Hollo G, Topouzis F, Fechtner RD. Fixed-combination intraocular pressure-lowering therapy for glaucoma and ocular hypertension: advantages in clinical practice. Expert Opin Pharmacother. 2014, 15(12): 1737-1747.

14. Clement CI, Bhartiya S, Shaarawy T. New perspectives on target intraocular pressure. Surv Ophthalmol. 2014, 59(6): 615-626.

15. Razeghinejad MR, Fudemberg SJ, Spaeth GL. The changing conceptual basis of trabeculectomy: a review of past and current surgical techniques. Surv Ophthalmol. 2012, 57(1): 1-25.

16. Hollows FC, Graham PA. Intra-ocular pressure, glaucoma, and glaucoma suspects in a defined population. Br J Ophthalmol. 1966, 50(10): 570-586.

17. Anderson DR. Normal-tension glaucoma (Low-tension glaucoma). Indian J Ophthalmol. 2011, 59 Suppl: S97-101.

18. Drance SM. Some factors in the production of low tension glaucoma. Br J Ophthalmol. 1972, 56(3): 229-242.

19. Levene RZ. Low tension glaucoma: a critical review and new material. Surv Ophthalmol. 1980, 24(6): 621-664.

20. Shields MB. Normal-tension glaucoma: is it different from primary open-angle glaucoma? Curr Opin Ophthalmol. 2008, 19(2): 85-88.

21. Greenfield DS, Liebmann JM, Ritch R, Krupin T. Visual field

and intraocular pressure asymmetry in the low-pressure glaucoma treatment study. Ophthalmology. 2007, 114(3): 460-465.
22. Bae HW, Lee N, Lee HS, Hong S, Seong GJ, Kim CY. Systemic hypertension as a risk factor for open-angle glaucoma: a meta-analysis of population-based studies. PLoS One. 2014, 9(9): e108226.

23. Jonas JB, Yang D, Wang N. Intracranial pressure and glaucoma. J Glaucoma. 2013, 22 Suppl 5: S13-S14.

24. Comoglu S, Yarangumeli A, Koz OG, Elhan AH, Kural G. Glaucomatous visual field defects in patients with migraine. J Neurol. 2003, 250(2): 201-206.

25. Pang JJ, Gao F, Wu SM. Light responses and morphology of bNOS-immunoreactive neurons in the mouse retina. J Comp Neurol. 2010, 518(13): 2456-2474.

26. Pang JJ, Wu SM. Morphology and immunoreactivity of retrogradely double-labeled ganglion cells in the mouse retina. Invest Ophthalmol Vis Sci. 2011, 52(7): 4886-4896.

27. Pease ME, Hammond JC, Quigley HA. Manometric calibration and comparison of TonoLab and TonoPen tonometers in rats with experimental glaucoma and in normal mice. J Glaucoma. 2006, 15(6): 512-519.

28. Cook JE, Becker DL. Gap junctions in the vertebrate retina. Microsc Res Tech. 1995, 31(5): 408-419.

29. Mills SL, Massey SC. Differential properties of two gap junctional pathways made by AII amacrine cells. Nature. 1995, 377(6551): 734-737.

30. Vaney DI, Nelson JC, Pow DV. Neurotransmitter coupling through gap junctions in the retina. J Neurosci. 1998;18(24): 10594-10602.

31. Mrini A, Moukhles H, Jacomy H, Bosler O, Doucet G. Efficient immunodetection of various protein antigens in glutaraldehyde-fixed brain tissue. J Histochem Cytochem. 1995, 43(12): 1285-1291.

32. Libby RT, Anderson MG, Pang IH, Robinson ZH, Savinova OV et al. Inherited glaucoma in DBA/2J mice: pertinent disease features for studying the neurodegeneration. Vis Neurosci. 2005, 22(5): 637-648.

33. Sit AJ. Intraocular pressure variations: Causes and clinical significance. Can J Ophthalmol. 2014, 49(6): 484-488.

34. Stamer WD, Acott TS. Current understanding of conventional outflow dysfunction in glaucoma. Curr Opin Ophthalmol. 2012, 23(2): 135-143.

35. Glovinsky Y, Quigley HA, Dunkelberger GR. Retinal ganglion cell loss is size dependent in experimental glaucoma. Invest Ophthalmol Vis Sci. 1991, 32(3): 484-491.

36. Glovinsky Y, Quigley HA, Pease ME. Foveal ganglion cell loss is size dependent in experimental glaucoma. Invest Ophthalmol Vis Sci. 1993, 34(2): 395-400.

37. Harwerth RS, Carter-Dawson L, Shen F, Smith EL, III, Crawford ML. Ganglion cell losses underlying visual field defects from experimental glaucoma. Invest Ophthalmol Vis Sci. 1999, 40(10): 2242-2250.

38. John SW, Smith RS, Savinova OV, Hawes NL, Chang B et al. Essential iris atrophy, pigment dispersion, and glaucoma in DBA/2J mice. Invest Ophthalmol Vis Sci. 1998, 39(6): 951-962.

39. Moon JI, Kim IB, Gwon JS, et al. Changes in retinal neuronal populations in the DBA/2J mouse. Cell Tissue Res. 2005, 320(1): 51-59.

40. Ahmed SM, Rzigalinski BA, Willoughby KA, Sitterding HA, Ellis EF. Stretch-induced injury alters mitochondrial membrane potential and cellular ATP in cultured astrocytes and neurons. J Neurochem. 2000, 74(5): 1951-1960.

41. Almasieh M, Wilson AM, Morquette B, Cueva Vargas JL, Di PA. The molecular basis of retinal ganglion cell death in glaucoma. Prog Retin Eye Res. 2012, 31(2): 152-181.

42. Burgoyne CF, Downs JC. Premise and prediction-how optic nerve head biomechanics underlies the susceptibility and clinical behavior of the aged optic nerve head. J Glaucoma. 2008, 17(4): 318-328.

43. Frankfort BJ, Khan AK, Tse DY, Chung I, Pang JJ et al. Elevated intraocular pressure causes inner retinal dysfunction prior to cell loss in a mouse model of experimental glaucoma. Invest Ophthalmol Vis Sci. 2012, 54(1): 762-70.

44. Martin JL, McCutcheon SC. Hydrodynamics and Transport for Water Quality Modeling. 1st ed. Boca Raton: CRC Press; 1998.

45. Duff W, Carman AP, Lewis P, McClung RK. A textbook of physics. 4th edition ed. Philadelphia: Philadelphia P. Blakistons son & Co.; 1916:110-115.

46. Sadd MH. Elasticity, Second Edition: Theory, Applications, and Numerics. 2nd ed.: Academic Press; 2009.

47. Goel M, Picciani RG, Lee RK, Bhattacharya SK. Aqueous humor dynamics: a review. Open Ophthalmol J. 2010, 4: 52-59.

48. Brown CT, Vural M, Johnson M, Trinkaus-Randall V. Age-related changes of scleral hydration and sulfated glycosaminoglycans. Mech Ageing Dev. 1994, 77(2): 97-107.

49. Howell GR, Libby RT, Jakobs TC, Smith RS, Phalan FC et al. Axons of retinal ganglion cells are insulted in the optic nerve early in DBA/2J glaucoma. J Cell Biol. 2007, 179(7): 1523-1537.

50. Danias J, Lee KC, Zamora MF, Chen B, Shen F et al. Quantitative analysis of retinal ganglion cell (RGC) loss in aging DBA/2NNia glaucomatous mice: comparison with RGC loss in aging C57/BL6 mice. Invest Ophthalmol Vis Sci. 2003, 44(12): 5151-5162.

51. Leidl MC, Choi CJ, Syed ZA, Melki SA. Intraocular pressure fluctuation and glaucoma progression: what do we know? Br J Ophthalmol. 2014, 98(10): 1315-1319.

52. Caiado RR, Badaro E, Kasahara N. Intraocular pressure fluctuation in healthy and glaucomatous eyes: a comparative analysis between diurnal curves in supine and sitting positions and the water drinking test. Arq Bras Oftalmol. 2014, 77(5): 288-292.

53. Quigley HA. Neuronal death in glaucoma. Prog Retin Eye Res. 1999, 18(1): 39-57.

54. Yanagi M, Kawasaki R, Wang JJ, Wong TY, Crowston J et al. Vascular risk factors in glaucoma: a review. Clin Experiment Ophthalmol. 2011, 39(3): 252-258.

55. Akagi T, Hangai M, Takayama K, Nonaka A, Ooto S et al. In vivo imaging of lamina cribrosa pores by adaptive optics scanning laser ophthalmoscopy. Invest Ophthalmol Vis Sci. 2012, 53(7): 4111-4119.

56. Rogers RS, Dharsee M, Ackloo S, Sivak JM, Flanagan JG. Proteomics analyses of human optic nerve head astrocytes following biomechanical strain. Mol Cell Proteomics. 2012, 11(2): M111.

57. Ostrow LW, Langan TJ, Sachs F. Stretch-induced endothelin-1 production by astrocytes. J Cardiovasc Pharmacol. 2000, 36(5 Suppl 1): S274-S277.